

Iris Recognition System using Polar Spline RANSAC based on Total Variation Model

Zainab Ghayyib Abdul Hasan¹, Alyaa Mohsin Dhayea², Esraa H. Abdul Ameer³

Submitted: 10/11/2022

Accepted: 12/02/2023

Abstract: A biometric system allows an individual to be automatic identification using a distinguishing or single feature possessed by the person. The biometric system of identification available which is regarded as the most accurate and reliable known is iris recognition. In this paper, we discuss the strategies used to construct an Iris Recognition System, as well as an analysis of our findings. To locate the limits of the iris in the digital image of the human eye, we used an integration procedure that incorporated both a Polar Spline RANSAC and a Total Variation Model. Predictable patterns of an individual's iris are retrieved as a feature vector using Daugman's rubber sheet model and the Gabor filter. The quantified values are then compared using the Hamming Distance operator to see whether the two irises are really the same. Experiments demonstrated that the accuracy of the recommended strategy for photographs acquired in uncooperative situations is either superior to or equivalent to other ways provided in the literature.

Keywords: Iris recognition, Segmentation, image processing, Biometric identification, Polar Spline RANSAC, Total Variation Model

1. Introduction

The term biometrics tends to refer to science that studies biological features statistically. Biometrics is employed here for security purposes to analyze human features. These Biometric characteristics can be physical, like voice, hand, retina vessel, fingerprint, eye, and face or behavioural, such as typing rhythm and signature. For the time being, the most essential factor in the domain of the military, e-commerce, business, information, etc is security. As a result, individual identification is becoming an important subject. Several preceding approaches used for identification are passwords, PIN (Personal Identification Number), signatures, and ID cards which are utilized vastly, and have Several downsides [1] [2]. PIN or ID card can be stolen, signatures may be imitated and passwords can be forgotten. To tackle these issues used Biometric characteristics. Patterns of retinal blood vessels, voiceprints, and fingerprints can be used as an alternative to non-biometric techniques for more reliability and safety. The goal of Iris Recognition, a biometric-based technique for person verification and identification, is to identify an individual from her/his iris prints. Iris patterns, in reality, have a greater standard of distinctiveness and stability. Each person has a distinct iris (see Figure 1); Even between the left and right eyes of the same person and between identical twins, there are variances. [3]

2. History

Alphonse Bertillon, a French ophthalmologist, appears to have

*1*Department of Computer Science, Faculty of Education for Girls, University of Kufa, Iraq, ORCID ID:0000-0002-1674-0690

2 Department of Computer Science, Faculty of Archaeology, University of Kufa, Iraq

*3*Department of Computer Sciences, Faculty of Education for Girls, University of Kufa, Iraq

* Corresponding Author Email: zainabg.alhatimy@uokufa.edu.iq

been the first to propose using iris pattern (colour) as a foundation for personal identification [4]. In 1981, Aran Safir and Flom proposed utilizing the iris as the foundation for a biometric. In 1991, John Daugman [5] after collaborating with Safir and Flom for four years introduced and developed the application and use for individual identification of iris as a biometric feature. To acquire the 2048 binary feature code, he utilized 2D Gabor filters and phase coding and successfully tested his technique on numerous images. Next his work, other people suggested different structures for iris recognition. Wilds [6] utilized 4- level resolutions and Laplacian pyramids. His algorithm requires many computations which depend on image registration and matching. For the purposes of the Boles model [7], the grey-level profiles of the iris are represented in a single dimension. After applying the wavelet transform to one dimension, he used the representation at the zero crossing. Wang, Ma, and Tang [8] [9] explored a class of Gabor Filters in a number of publications. To demodulate the iris's texture, Tisse et al. [10] produced an analytical image (incorporation of its Hilbert transform and the original image). Woo Nam et al. Lim et al. [12] employed quantized fourth-level high-frequency information and a two-dimensional Haar wavelet to generate a feature vector with an 87-binary code length and an LVQ neural network for classification. Multilayer perceptron with modified Haralick's co-occurrence style is also presented for iris extraction and classification [13] [14].

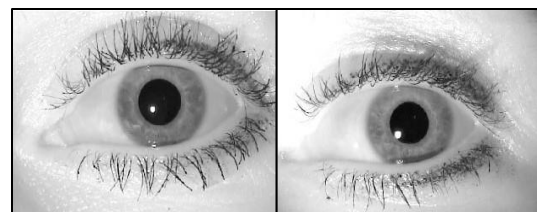


Fig 1. Distinctiveness of human iris

3. Methodology

In this research, we offer an effective approach for iris-based personal identification. The suggested recognition system comprises iris segmentation, normalization, feature extraction, and matching after the image capture process. Preprocessing to

eliminate noise, iris internal boundary estimate, iris exterior boundary estimation, and estimation of the circles indicating the iris area boundaries are the iris segmentation phases. Figure 2 illustrates a comprehensive block design of the proposed iris recognition system. The processes of the iris recognition system are discussed in detail below.

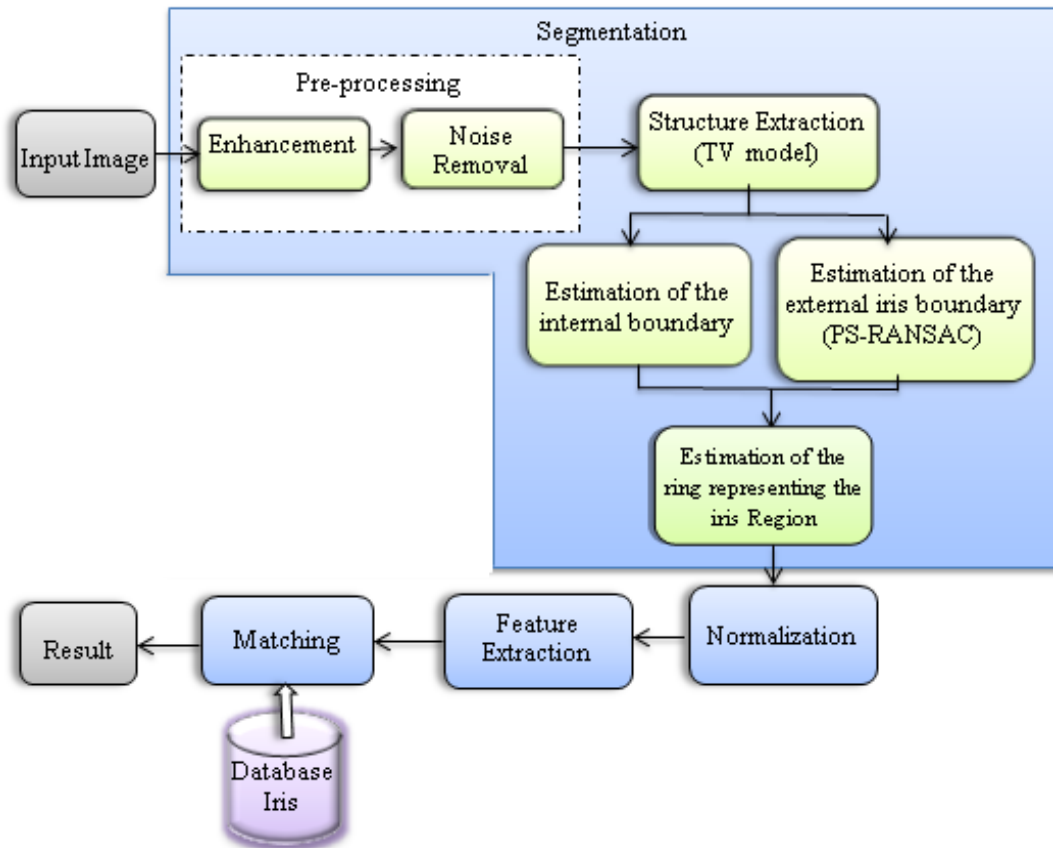
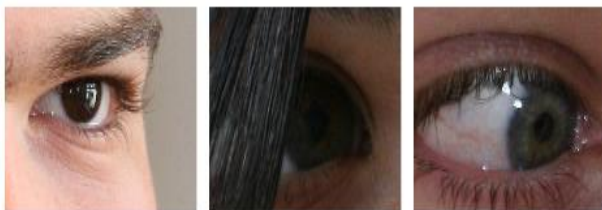


Fig 2. The block diagram of the proposed iris recognition model

4. Segmentation

In this paper, we propose the Polar Spline RANSAC and Total Variation Model, An effective technique for iris segmentation in uncooperative ocular images, where the iris shape is approximated as a closed curve with arbitrary degrees of freedom. As seen in Figure 3, the approach is robust against nonidealities such as occlusions, pupil dilation, poor focus, variations in image resolution, shadows, low contrast, gaze deviations, shadows, differences in image resolution, and motion blur in nonideal images. The proposed method, unlike other strategies in the literature, performs well under difficult situations with a variety of imaging wavelengths. We also research how different lighting adjustment approaches affect the iris segmentation process.



(a) (b) (c)

Fig 3. Examples of UBIRIS v.2 database: (a) small iris diameter, (b) occlusions, and (c) gaze deviation.

4.1. Preprocessing

Several factors, such as the illumination source angle and changing illumination intensity, can have a negative influence on the quality and accuracy of iris segmentation in less-constrained imaging. Such unanticipated varying yield some challenges not just in iris biometrics but also in a variety of other image comprehension tasks. For normalizing the illumination of the eye image, we utilized the Single Scale Retinex (SSR) technique [15]. The SSR improvement technique can enhance colour intensity in the presence of significant illumination variation. Figure 4 shows an example image after using SSR improvement. The median filter is used on the image after improvement to eliminate isolated noisy pixels.



Fig 4. Example of the image from the preprocessing step: (a) the input image, (b) improved image, (c) smoothed red channel.

4.2. Structure Extraction(Total Variation Model)

Eye photographs captured in less-than-ideal conditions are notorious for their susceptibility to noisy and complicated properties like eyelashes and reflection, which are superfluous for the first structural analysis. To combat the issue of ambiguous variance of structural components and growing noise interference, we used the total variation (TV) model [16]. The pupil circle represents the circular boundaries that roughly correspond to the pupillary borders images of the iris produced during segmentation. Using this method, we can dependably extract the structure of the eye for further segmentation through more precisely localizing circles of the pupil. The algorithm enhances the resistance to irregularly shaped borders influenced by reflections and noise. In reality, colour images typically have a large iris-sclera contrast, allowing for a relatively accurate estimation of the iris area. This energy regularizer has superior performance in some applications and has more crucial geometric features, which is deemed advantageous for the following iris localization procedure. Figure 5 shows an example of Total Variation model findings for eye images under visible light.

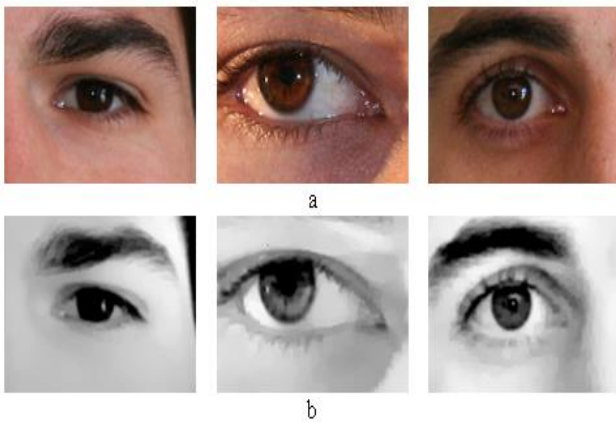


Fig 5.The results of the structure extraction stage using total variation model (a)input images (b) of structure extraction for eye images

4.3. Iris internal boundary estimation

It is not possible to use a simple circular model to segment iris images obtained in a less controlled setting. However, the human iris may be thought of as a roughly round shape [5] [18]. To further refine the iris segmentation borders, a series of effective post-processing methods may be utilized to create a circular border that roughly but closely fits the limbic boundary. A coarse localization circle is called an iris circle in this research. Pupil circles, on the other hand, are made out of circular borders that match the pupillary boundary of segmented iris images quite well. The circular Hough transform (CHT) based technique may be utilized to identify the iris and pupil circles coarsely after structure extraction has greatly decreased the noise in eye images. Based on the two-phase CHT described in [19], we created an enhanced version of CHT. The enhanced CHT increases the strength for coarsely localizing the iris area. Figure 6(a) shows examples of an estimated internal iris boundary are presented. [35, 120] is the radius possible ranges for the database we utilized, UBIRIS.v2.

4.4. Iris External Boundary Estimation(Ps-Ransac)

In this step, we refine the boundary shape using various RANSAC [20, 21] to estimate the points on the iris's periphery. We do this by looking for the highest values obtained when a radial-gradient-based operator is applied to the image R_E . In the

first step, we take a look at the input image R_E and calculate the boundary points vector E_B that represents the outside world. This is accomplished by acquiring the coordinates of polar points with the greatest values using a gradient-based operator. Image I_P is computed by translating R_E to polar coordinates with the pupil centroid as the center and a radial resolution of 1° (360 columns). Because the inner edge of the iris is often more contrasted than the outside edge, the image I_P is computed starting with a minimal radius r_{min} , and the dataset to be studied is experimentally calibrated. To better highlight the continuous segment denoting the iris's limits, we employ our gradient-based operator. When compared to gradient-based methods, this operator is meant to lessen the obstructive effects of the eyelids in the following way:

$$I_G(\theta, \rho) = I_P(\theta, \rho) * m(\theta', \rho'), \quad (1)$$

Where the mask is $4 \times N$ represent m can be defined as follows:

$$m(\theta', \rho') = \begin{cases} 1 & \text{if } y_m > 2, \\ 0 & \text{otherwise,} \end{cases} \quad (2)$$

Where $*$ is the convolution operator and the y coordinate of the mask m is y_m . The radius corresponded for each angle θ is calculated as follows:

$$\begin{aligned} X(\theta) &= \operatorname{argmax}[I_G(\theta, \rho)], \\ \rho &= 1 \dots P \end{aligned} \quad (3)$$

Where P denotes the image size (I_G) along the axis(ρ). A sample of an estimated external border X is shown in Figure 6(b). In this technique, the second task for external border segmentation includes refinement of the estimated iris contour shape utilizing a RANSAC-based algorithm. In segmentation implementations, PS-RANSAC can be utilized to suitable a collection of candidate points of boundary via eliminating outliers. In the segmentation technique of the iris, the iris boundaries are approximated by PS-RANSAC as closed curves with freedom of arbitrary degrees.

4.5. Estimation of The Circles Representing The Iris Region Limits

In the proposed iris segmentation method, the iris's boundaries are represented by curves with arbitrary degree freedom. Traditional iris detection systems, such the one presented in Daugman (2002) [5], have several drawbacks. The iris region has to be limited such that a scale-invariant representation of the iris area may be built using two circles (Rubber Sheet Model). The suggested approach, when applied to such setups, derives the circular inner iris boundary from the shape defining the outer irises. To supply a robust representation of the iris shape, our technique excludes points from the vector E_R that correspond to the contours of the eyelashes and eyelids, which represents the refined coordinates of the external boundary, and then uses the remaining coordinates to perform circle fitting utilizing the mean-square method, so the algorithm only examines points in E_R with coordinates in the ranges $[-10^\circ, \dots, 40^\circ]$ and $[140^\circ, \dots, 90^\circ]$.

5. Database Ubiris.V2

Database Ubiris.v2 consists of captured under unconstrained conditions samples on the move and in natural light illumination. Proenca et al. characterize it as

the second version of a subset of the Noisy Visible Wavelength Iris Image Databases (UBIRIS.v2) [22]. (2010). This database is considered challenging owing to its utilization of several literary works, such as Alexandre and Proenca (2007). The images coincide with right and left eyes, have been taken under unconstrained conditions and in visible light, and have a size of 400x300 pixels.

The acquisitions were made while moving at a distance ranging from four to eight meters from the camera. Reflections, occlusions, blur and off-angle are all significant nonidealities in ocular images. Figure 3 depicts non-ideal photos obtained with a digital single lens reflex digital camera in an unrestricted area, under natural lighting conditions, and at different camera distances. Each image has a resolution of 400 by 300 pixels.

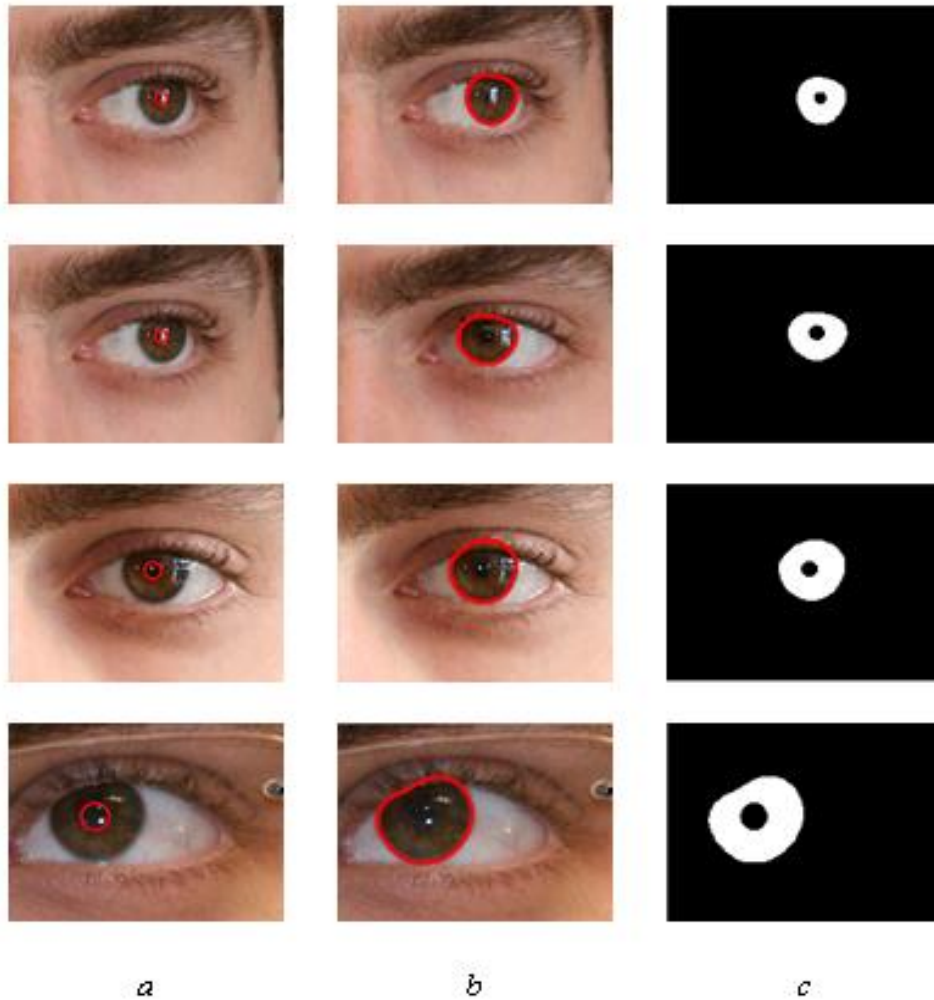


Fig 6. Examples of the results acquired utilizing the proposed segmentation algorithm (a) Ocular image and pupil parameters (b) External iris boundaries (c) Segmentation mask

6. Normalization

The next phase after successful segmentation of the iris boundary is the unwrapping of the segmented iris to fixed resolution. The circular iris image is converted into a rectangular image during the normalizing process. Utilizing Daugman's rubber sheet model, the circular intensities in the image of the iris are transformed to polar intensity. The point of the iris is remapped to the polar coordinates pair represented by (r, θ) into a Cartesian coordinate (x, y) during the normalization process by Daugman's Rubber Sheet Model [23]. The procedure is depicted in Figure 7. The transformation is performed via the following formulas.

$$\theta \in [0 \ 2\pi], \rho \in [0 \ 1], I(x(\rho, \theta), y(\rho, \theta)) \rightarrow I(\rho, \theta)$$

$$x(\rho, \theta) = (1 - \rho)x_p(\theta) + \rho x_i(\theta) \quad (4)$$

$$y(\rho, \theta) = (1 - \rho)y_p(\theta) + \rho y_i(\theta)$$

$$x_p(\theta) = x_{p0}(\theta) + r_p \cos(\theta) \quad (5)$$

$$y_p(\theta) = y_{p0}(\theta) + r_p \sin(\theta)$$

$$x_i(\theta) = x_{i0}(\theta) + r_i \cos(\theta) \quad (6)$$

$$y_i(\theta) = y_{i0}(\theta) + r_i \sin(\theta)$$

Where (ρ, θ) and (x, y) are the polar and normalized Cartesian coordinates respectively, $I(x, y)$ is the iris region, (x_i, y_i) and (x_p, y_p) are coordinates on limbus and pupil boundaries along the θ direction, $(x_{i0}, y_{i0}), (x_{p0}, y_{p0})$ are the coordinates of iris and pupil centers [1].

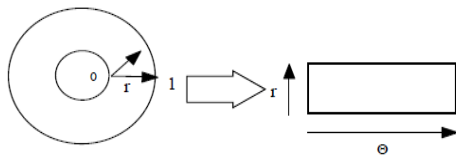


Fig 7. Daugman's Rubber Sheet Model

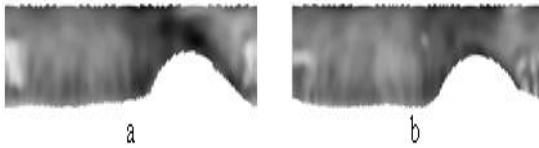


Fig 8. Normalization iris image of two different eyes (a,b)

7. Feature Encoding (Gabor Filters)

The feature encoding was carried out by convolving a normalized iris pattern with 1D Log-Gabor wavelets. First, the 2D normalized pattern is partitioned into a series of 1D signals before being convolved with the 1D Gabor wavelets. Each row in the 2D normalized pattern represents one of the iris's rings, and together they make up the 1D signal. Since the columns of the normalized pattern are oriented radially, we choose the angular direction instead since it has a higher degree of independence. [25]

The intensity values in locations with known noise are normalized to the average intensity of the surrounding pixels in the pattern, which eliminates the effect of the noise on the filtering result. Next, the filtered data is phase-quantized into four levels using the Daugman method [5], with each filter producing two bits of data for each phasor. Phase quantization's result is a gray code, with just one bit shifting from one quadrant to the next. By reducing the number of bits that disagree, detection accuracy is improved if two intra-class patterns are just slightly out of sync with one another. The method of encoding creates a noise mask that corresponds to the incorrect locations in the iris pattern, which is based on a bitwise template consisting of information bits. There is no use in storing phase information in regions of zero amplitude, hence these areas are likewise labeled in the noise mask. The total number of bits in the template is calculated as the product of the radial resolution times the angle resolution times 2 times the number of filters [2]. The results of the iris feature code are shown in Figure 9.

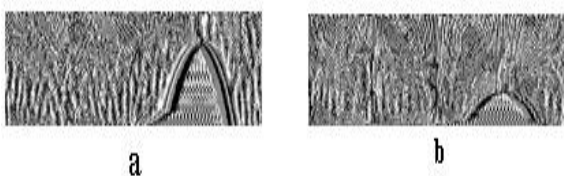


Fig. 9. Iris feature code of two different eyes (a,b)

8. Template Matching (Hamming Distance)

The Hamming distance was used as the recognition matching measure because to the need for bit-wise comparisons. The Hamming distance method was used to determine how similar or different two iris patterns were, and noise masking was used into the process. The Hamming distance will be calculated using just the bits of the iris pattern that have the same value as the '0' bits in both noise masks. When calculating the Hamming distance, we

now use the bytes that result from the iris's real area, and we provide the formula for this revised measure [25].

$$HD = \frac{1}{N} \sum_{j=1}^N X_j(XOR)Y_j \quad (7)$$

Where the two bit-wise templates are Y_j and X_j to compare and the number of bits is N that represented via each template. Although in theory two identical iris templates would have a hamming distance of zero, this is unlikely to occur in practice. There will be certain dissimilarities between any two iris intra-class templates. Reason being that Normalization isn't perfect and some noise will sneak through undetected. To account for rotational abnormalities, the Hamming distance between two templates will be computed using a bit-wise shift to the left and right for one of the templates. The horizontal bits are shifted in a manner that is proportional to the angular resolution used, which in turn is proportional to the starting rotation of the iris area. For the iris, a 180-degree resolution translates to a 2-degree rotation with each shift. Using a normalized iris pattern, as described by Daugman [26], this method fixes alignment discrepancies brought on by rotational fluctuations in the imaging process. As this represents the highest degree of similarity between the two templates, only the smallest of the Hamming distance values is used.

9. Experimental Results

9.1. Segmentation Accuracy

Using the same technique as the NICE. I competition [26], the average segmentation error rate is calculated as follows:

$$\bar{e} = \frac{1}{N \times w \times h} \sum_{x \in w} \sum_{y \in h} t(x,y) \oplus m(x,y) \quad (8)$$

The total number of images is N , where h and w are the height and breadth of one image, m and t are the produced iris mask and ground truth mask, respectively. The symbol \oplus symbolizes an exclusive OR operation for segmentation error identification. While ground truth for UBIRIS.v2 is manually tagged and made available to the public by NICE.I. Therefore, the NICE.I technique may be used to evaluate segmentation accuracy consistently. The suggested method produced segmentation error rates of 0.89 per cent on average for UBIRIS.v2. PS-RANSAC demonstrated the highest identity verification accuracy and pixel-wise classification accuracy for non-ideal photos acquired under visible light illumination, similar to contemporary techniques based on deep learning and algorithms created expressly for this group of data.

9.2. Recognition Performance

In iris recognition systems, recognition performance is always the top priority. To determine if our precise iris segmentation method may also assist in enhancing recognition performance. we tested our method using the UBIRIS.v2 Database. We tested our project on 1000 images that are collected from 100 individuals, each individual has 10 images, from the first session 5 images and from the second session 5 images. We obtained a recognition rate of 99.66%. We compared the acquired results with other approaches in the publicly available software and literature. In table 1 a comparison between some previous works and our method is shown [26]. For samples gathered under less-than-ideal conditions and acquired with infrared illuminators, the proposed method yielded the highest identity verification precision.

Table 1. Comparison of our suggested method's results with the other existing methods

Method	Accuracy rate %
Proposed method	99.66
Sangeetha [27]	98.75
Zhao et al. [28]	89
Ahmadi and Akbarizadeh [29]	88.24
Oktiana et al. [30]	87.9
Nguyen et al. [31]	87.16
Christian et al. [32]	78.36

10. Conclusions

In this study, a robust approach to iris recognition is proposed. The iris and pupil are identified using the Total Variation Model and Polar Spline RANSAC in this system. The Daugman rubber sheet model achieves normalization. The Gabor filters are utilized for feature extraction. The Hamming Distance is utilized to determine if a person is authorized or unauthorized. The experiment utilizing various illumination compensation strategies shows that an algorithm based on the Retinex model provides identification accuracy and improved segmentation. When processing non-ideal ocular images emphasize the necessity of applying illumination models. This system gives 99.66% Accuracy on the UBIRIS.V2 database. This study shows more accuracy & better performance as compared to other iris recognition systems for images obtained in non-ideal conditions in the literature.

References

- [1] Daugman, J., "Complete Discrete 2-D Gabor Transforms by Neural Networks for Image Analysis and Compression", IEEE Transactions on Acoustics, Speech, and Signal Processing, Vol. 36, no. 7, July 1988, pp. 1169-1179.
- [2] Daugman, J., "High Confidence Visual Recognition of Persons by a Test of Statistical Independence," IEEE transactions on pattern analysis and machine intelligence, vol. 15, no.11, November 1993, pp. 1148-1161.
- [3] Wildes, R.P, "Iris Recognition: An Emerging Biometric Technology", Proceedings of the IEEE, VOL. 85, NO. 9, September 1997, pp. 1348-1363.
- [4] A. Bertillon, "la couleur de l'iris, Revue scientifique", France, 1885.
- [5] J. Daugman, "How Iris Recognition Works", Proceedings of 2002 International Conference on Image Processing, Vol. 1, 2002.
- [6] R.P. Wildes, Asmuth, J.C. et al., "A System for Automated Iris Recognition", Proc of the Second IEEE Workshop on Applications of Computer Vision, 1994, pp.121 -128.
- [7] W.W. Boles and B. Boashash, "A Human Identification Technique Using Images of the Iris and Wavelet Transform", IEEE Trans. on Signal Processing, 46(4), 1998, pp.1185-1188.
- [8] L. Ma, Y. Wang, and T. Tan, "Personal Identification Based on Iris Texture Analysis", IEEE Transaction on pattern analysis and machine intelligence, vol. 25, no. 12, December 2003.
- [9] L. Ma, Y. Wang, and T. Tan, "Iris Recognition Using Circular Symmetric Filters", Proc. 16th Int'l Conf. Pattern Recognition, vol. II, pp. 414-417, 2002.
- [10] C. Tisse, L. Martin, L. Torres and M. Robert, "Person identification technique using human iris recognition", St Journal of System Research , 2003, Vol. 4, pp. 67-75.
- [11] K.W. Nam, K. L. Yoon, J. S. Bark, W. S. Yang, "A feature extraction method for binary iris code construction", Proceedings of the 2nd International Conference on Information Technology for Application (ICITA 2004).
- [12] S. Lim, K. Lee, O. Byeon and T. Kim, "Efficient Iris Recognition through Improvement of Feature Vector and Classifier", ETRI Journal, Volume 23, Number 2, June 2001.
- [13] P. Jaboski, R. Szewczyk, Z. Kulesza, et. al., "Automatic People Identification on the Basis of Iris Pattern Image Processing and Preliminary Analysis", Proc. Int. Conf. on Microelectronics (MIEL 2002), VOL 2, Yugoslavia pp. 687-690, May, 2002.
- [14] R. Szewczyk, P. Jaboski, et. al., "Automatic People Identification on the Basis of Iris Pattern - Extraction Features and Classification", Proc. Int. Conf. on Microelectronics (MIEL 2002), VOL 2, Yugoslavia pp. 691-694, May, 2002.
- [15] D. H. Brainard and B. A. Wandell, "Analysis of the retinex theory of color vision", J. Optical Soc. Am. A, vol. 3, no. 10, pp. 1651-1661, 1986.
- [16] Zhao, Zijing, and Kumar Ajay. "An accurate iris segmentation framework under relaxed imaging constraints using total variation model", Proceedings of the IEEE international conference on computer vision. 2015.
- [17] A. Kumar and A. Passi, "Comparison and combination of iris matchers for reliable personal authentication", Pattern Recognition, vol. 43, no. 3, pp. 1016-1026, 2010.
- [18] E. R. Davies. "Circle and ellipse detection", in Computer and Machine Vision, Fourth Edition: Theory, Algorithms, Practicalities, Waltham: Academic Press, 2012.
- [19] Kim, T., and W. Yu. "Performance evaluation of ransac family", Proceedings of the British Machine Vision Conference (BMVC). 2009.
- [20] Wang, Kai, and Yuntao Qian. "Fast and accurate iris segmentation based on linear basis function and ransac", 2011 18th IEEE International Conference on Image Processing. IEEE, 2011.
- [21] H. Proenca, S. Filipe, R. Santos, J. Oliveira, and L. A. Alexandre, "The UBIRIS. v2: A database of visible wavelength iris images captured on-the-move and at-a-distance", IEEE Trans. Pattern Anal. Mach. Intell., vol. 32, no. 8, pp. 1529-1535, 2010.
- [22] Daugman, John G. "Biometric personal identification system based on iris analysis", U.S. Patent No. 5,291,560. 1 Mar. 1994.
- [23] Das, Animesh. Recognition of Human Iris Patterns. Diss. 2012.
- [24] Masek, Libor. Recognition of human iris patterns for biometric identification. Diss. Master's thesis, University of Western Australia, 2003.

- [25] Sanderson, S., and J. H. Erbetta. "Authentication for secure environments based on iris scanning technology", (2000): 8-8.
- [26] NICE.I-Noisy Iris Challenge Evaluation, Part I. <http://nice1.di.ubi.pt/>.
- [27] A. Antony Chrisda Lina and B. Sivagami, "A DEEP SURVEY ON IRIS RECOGNITION METHODS", *Journal of Information and Computational Science*, vol. 10, no. 1, 2020.
- [28] Sangeetha, S. Pon. "Fusion of local and global iris features to construct feature vector using genetic algorithm", *International Journal Of Computer Science And Information Technologies*. 6.2 (2015): 1486-1489.
- [29] Zhao, Tianming, et al. "A deep learning iris recognition method based on capsule network architecture", *IEEE Access* 7 (2019): 49691-49701.
- [30] Ahmadi, Neda, and Gholamreza Akbarizadeh. "Hybrid robust iris recognition approach using iris image pre-processing, two-dimensional gabor features and multi-layer perceptron neural network/PSO" *Iet Biometrics* 7.2 (2018): 153-162.
- [31] Oktiana, Maulisa, et al. "Advances in cross-spectral iris recognition using integrated gradientface-based normalization", *IEEE Access* 7 (2019): 130484-130494.
- [32] Nguyen, Kien, et al. "Iris recognition with off-the-shelf CNN features: A deep learning perspective", *IEEE Access* 6 (2017): 18848-18855.
- [33] Christian Rathgeb, Nicolas Buchmann, Heinz Hofbauer, Harald Baier, Andreas Uhl, Christoph Busch, "Methods for accuracy-preserving acceleration of large-scale comparisons in CPU-based iris recognition systems", *IET Biometrics*, vol. 7 , issue 4, pp. 365-36.
- [34] Wildes, Richard P. "Iris recognition: an emerging biometric technology".